Comparison of RANS and LES Turbulence Models against Constant Volume Diesel Experiments

S. Som[*1], P.K. Senecal[2], and E. Pomraning[2]
[1]Energy Systems Division, Argonne National Laboratory, Argonne, IL-60439, USA
[2]Convergent Science Inc., Middleton, WI-53562, USA

Abstract

Under modern direct injection diesel engine conditions, the spray and combustion processes are known to be mixing controlled. Large eddy simulations (LES) can potentially improve the predictive capability by better capturing the large scale mixing of ambient air with the fuel vapor. In the present study, a Smagorinsky based LES model is implemented in the commercial code called CONVERGE. The LES model is compared against a standard Reynolds-averaged Navier-Stokes (RANS) based RNG k-ε model which is routinely used for engine simulations. Validations are performed against experimental data from Sandia National Laboratories in a constant volume combustion chamber using diesel surrogates i.e., n-heptane and n-dodecane under both non-reacting and reacting conditions. Using adaptive grid resolution, minimum grid sizes of 250 μm and 125 μm were obtained for the RANS and LES cases respectively. Under non-reacting conditions, global spray characteristics are well predicted by both the turbulence models. However, the LES model clearly improves qualitatively the instantaneous fuel vapor distribution. Under reacting conditions, the Smagorinsky based LES model better predicts the ignition delay characteristics compared to the RANS model. Flame stabilization phenomenon is also qualitatively accurately predicted with the LES model. However, these improved predictions come at an increased in computational cost. Sensitivity analysis was also performed to the LES model constants.

[*]Corresponding author: ssom@anl.gov

INTRODUCTION

Combustion in direct-injection diesel engines occurs in a lifted, turbulent diffusion flame mode. Numerous studies indicate that the combustion and emissions in such engines are strongly influenced by the lifted flame characteristics, which are in turn determined by fuel and air mixing in the upstream region of the lifted flame, and consequently by the liquid breakup and spray development processes [1-5]. They involve transient, two-phase turbulent flows with elevated pressures, and a wide range of temporal and spatial scales. These processes clearly play a critical role in determining the engine combustion and emission characteristics. For instance, correlation was observed between the soot distribution and lift-off length (LOL) for diesel jets in the recent experiments by Pickett and Siebers [6,7]. Consequently, the experimental, theoretical, and computational studies of these flows have been challenging. From a numerical standpoint, these spray combustion processes depend heavily on the choice of underlying spray, combustion, and turbulence models.

Fuel air mixing is non-uniform mainly due to the transient turbulent nature of the flow inside the combustion chamber. Subsequently, local inhomogeneity in equivalence ratio can result in varied ignition and emission characteristics [8]. Direct Numerical Simulations (DNS) offer potential to completely resolve all the relevant flow scales, however, the computational cost associated is not practical for engine studies [9]. Reynolds Averaged Navier Stokes (RANS) and more recently Large Eddy Simulation (LES) based approaches are typically employed for engine simulations. RANS approach is based on ensemble averaged governing equations, hence, cannot predict the local unsteadiness in the flow. LES approach which is based on spatially filtered governing equations can capture the large scale flow structures based on the filter size. However, the unresolved small scale structures are still modeled. Since LES can capture local unsteadiness and is computationally more tractable than a DNS based approach, it has received significant attention in the past decade, especially for simulation of internal combustion engines. An excellent review of different LES modeling approaches can be found in literature by Pope [10].

Our literature study reveals several groups using a RANS based approach [4,11-17]. In general, the global flow characteristics such as spray and vapor penetration, liquid length, ignition delay, flame lift-off length, heat release rates, and pressure traces etc., can be fairly well predicted by a RANS approach. This is not surprising since these global experimental parameters are reported in an ensemble averaged fashion [1,2,3]. More recently different flavors of LES models have been applied; an excellent reviews can be found in literature by Rutland [18]. Broadly they can be classified as viscosity and non-viscosity based. Pomraning [19,20] implemented a one equation non-viscosity dynamic structure model since it is known to be less dissipative compared to the viscosity based models, especially for coarse grids. Banerjee et al. [21], applied this model together with a sub-grid mixing model to predict the combustion characteristics under low-temperature conditions.

While different flavors of LES models have been used for predicting combustion and emission characteristics their ability to predict LOLs and ignition delays in constant volume combustion vessels has not been adequately assessed. Since diesel spray combustion processes are mixing controlled, improvements in predicting LOLs and ignition delays may be achieved with a LES model. This potential is the basis for the present numerical study, the primary objectives of which are to (1) Implement a Smagorinsky [22] based LES model in the commercial code CONVERGE (2) compare the RANS and LES approaches under both non-reacting and reacting conditions for qualitatively and quantitatively predicting the spray and flame structures. Another objective of this study is to assess the computational cost associated with running high resolution LES model. Smagorinsky based LES model is a viscosity based approach hence, is expected to be diffusive in nature on coarse grids. This drawback is partially circumvented by using grid sizes in the order of nozzle diameter. Another weakness of this model is that it is purely dissipative and does not allow for energy transfer from the sub-grid to the resolved scales. The authors intend to test the simplest implementation of an LES model before testing more advanced approaches. Hence the Smagorinsky based approach is selected for this computational study.

In the past decade, several studies were performed by researchers at Sandia National Laboratories to provide high-fidelity measurements of parameters such as spray penetration, liquid length, vapor penetration, mixture-fraction [23,24,25], ignition delay, LOL, and soot emissions for a range of ambient and injection conditions, in a constant volume combustion vessel. A variety of fuels and fuel surrogates, such as diesel #2, biodiesel, NHPT, and n-dodecane, were studied in these experiments, and the resulting dataset can be accessed through the Engine Combustion Network [26]. Only recently, this high-fidelity dataset has been used for spray combustion model development and validation. Of specific interest for the current study is the instantaneous fuel and temperature distribution measurements per-

formed by Idicheria et al. [23,24], since it provides more realistic information for LES model validation.

The paper is organized in the following way. First a brief introduction is provided for the spray and combustion models used followed by the governing equations for the Smagorinsky based LES model. The experimental dataset from Sandia National Laboratory which is extensively used for validation purposes is discussed next. The results and discussion section is mainly divided into non-reacting and reacting spray conditions. Robust validation of the Smagorinsky based LES model is provided and compared with predictions by the RANS model. The computational cost associated with standard RANS and high resolution LES approaches is also highlighted in this section. Finally, conclusions are presented.

PHYSICAL-COMPUTATIONAL MODEL

Fuel spray and combustion simulations were performed using the Eulerian-Lagrangian approach in the computational fluid dynamics software CONVERGE [4,27,28]. It incorporates state-of-the-art models for spray injection, atomization and breakup, turbulence, droplet collision, and coalescence. The gas-phase flow field is described by using either the Favre-Averaged Navier-Stokes equations in conjunction with the RNG k-ε or the LES based turbulence model, which includes source terms for the effects of dispersed phase on gas-phase turbulence. These equations are solved by using a finite volume solver. The details of these models can be found in previous publications [29], so only a brief description is provided here.

The Kelvin-Helmholtz (KH) and Rayleigh-Taylor (RT) models are used to predict the subsequent secondary droplet breakup [30,31]. Droplet collisions are modeled with no time counter algorithm [32]. Once a collision occurs, the outcomes of the collision are predicted as bouncing, stretching, reflexive separation, or coalescence [33]. A droplet evaporation model based on the Frossling correlation is used. Also used is a dynamic drag model based on the postulation that the drag coefficient depends on the shape of the droplet, which can vary between a sphere and a disk. The effects of turbulence on the droplet are accounted for using a turbulent dispersion model. It should be noted that for both RANS and LES based turbulence models, same set of spray constants was selected for validation purposes.

Detailed kinetic modeling is performed using the SAGE chemical kinetic solver [11,27,28] directly coupled with the gas-phase calculations using a well-stirred reactor model. The NHPT chemical kinetic mechanism used in the current study is from Lu and Law [34] consisting of 68 species and 283 elementary reactions. Several research groups are simultaneously working towards improving different aspects of turbulent spray combustion modeling. Our specific focus in this study is to improve the turbulence modeling by implementing a Smagorinsky based LES turbulence model. The authors are keenly following the developments in the field of turbulence chemistry interactions (TCI) modeling by Haworth et al. [35]. To the best of our knowledge this is the only group pursuing developments in TCI modeling for spray combustion applications. In a recent study by Haworth and co-workers [36], qualitative differences in the flame structure were observed between simulations accounting for TCI vs. not accounting for TCI. However, the reaction mechanisms chosen were that of n-heptane consisting of 29 and 34 species while the grid size was of the order of 1mm. The reaction mechanism used in the current study is two times higher in terms of number of species, the minimum grid size being 0.125mm. PDF based TCI modeling together with the large reaction mechanism and fine grid sizes used in the current study would be computationally too expensive and beyond the scope of the current study.

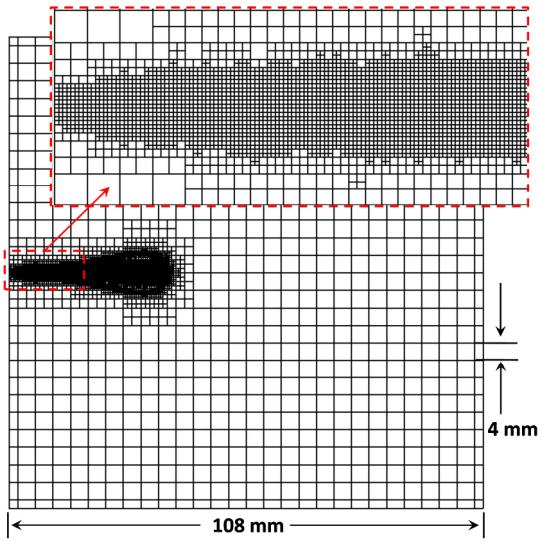

Figure 1: Grid generated in CONVERGE at 0.4 ms ASI for combusting spray simulations performed with a RANS model, described in Table 1. The field of view is 108 mm each side.

CONVERGE uses an innovative, modified cut-cell Cartesian method for grid generation [27,28]. The grid is generated internally at runtime. For all cases, the base grid size is fixed at 4 mm. In order to resolve the flow near the injector, a fixed grid em-

bedding is employed such that the minimum grid size is 0.25 mm for RANS and 0.125 mm for LES simulations. Apart from this region, it is rather difficult to determine *a priori* where a refined grid is needed. Hence, different levels of adaptive mesh refinement are employed for the velocity field. To match the combustion chamber geometry used in the experimental study, a cubical geometry of 108 mm on each side is generated (cf. Fig. 1). The zoomed-in view of the fixed embedding region is also shown. As mentioned earlier, the overall objective is to compare a standard RANS simulation against a higher-fidelity LES based approach under non-reacting and reacting conditions. The standard modeling approach consists of using a coarser minimum grid size with RANS based models (similar to studies reported in literature [4,11,12,14]), whereas, the high-fidelity approach consists of using a finer mesh (such as 0.125mm) with LES models. Smaller grid sizes were necessary with the LES model for two reasons: (1) since a zero-equation Smagorinsky model is being used, it is desirable that the sub-grid scale modeling is reduced, and (2) the possibility of accurately capturing the large-scale flow structures is higher with a finer grid.

LES – Smagorinsky Based Turbulence Model

Velocity and other thermodynamic variables are expressed in Favre form, whereas density and pressure are expressed in Reynolds form. The density-weighted LES spatial-filtering operation on the Navier-Stokes equation results in the filtered momentum equation:

$$\frac{\partial \overline{\rho}\tilde{u}_i}{\partial t} + \frac{\partial \overline{\rho}\tilde{u}_i\tilde{u}_j}{\partial x_j} = -\frac{\partial \overline{P}}{\partial x_i} - \frac{\partial \overline{\rho} T_{ij}}{\partial x_j} + \frac{\partial}{\partial x_j}\left(\mu \frac{\partial \tilde{u}_i}{\partial x_j}\right) - \overline{F_i} \quad (1)$$

where the LES sub-grid scale tensor:

$$T_{ij} = \left(\tilde{u_i u_j} - \tilde{u}_i \tilde{u}_j\right) \quad (2)$$

is modeled using a Smagorinsky-based model:

$$T_{ij} = -2C_s\Delta^2\left|\overline{S}\right|\overline{S_{ij}} + \frac{1}{3}\delta_{ij}T_{kk} \quad (3)$$

where $\left|\overline{S}\right| = \sqrt{2\overline{S_{ij}}\,\overline{S_{ij}}}$,

$$\Delta = V_{cell}^{1/3} \quad (4)$$

and $$\overline{S_{ij}} = \frac{1}{2}\left(\frac{\partial \overline{u_i}}{\partial x_j} + \frac{\partial \overline{u_j}}{\partial x_i}\right)$$

The spray models require a turbulent kinetic energy for closure. For the Smagorinsky model, the sub-grid turbulent kinetic energy is not readily available. Hence, the following expression is used for closure:

$$k \cong C_{les}\frac{\Delta^2}{24}\frac{\partial \overline{u_i}}{\partial x_j}\frac{\partial \overline{u_i}}{\partial x_j} \quad (5)$$

The influence of the two model constants C_s and C_{les} is investigated.

Experimental Data for Validation

Experimental data to use for comparison are obtained from Sandia National Laboratories, where a constant-volume, quiescent, pre-burn-type combustion vessel is used to generate high-temperature and high-pressure gases. A premixed combustible mixture is spark-ignited. The combustion products cool over a long time. Once the desired pressure and temperature are reached, the diesel fuel injector is triggered and fuel injection occurs. The conditions for both diesel fuel surrogates n-heptane and n-dodecane are noted in Table 1. The measured rate of injection (ROI) profile is top-hot for both the fuels and the total mass injected is also mentioned in the table. The liquid and vapor penetration versus time, liquid length, ignition delay and pressure-rise rate, LOL, and quantitative soot volume fraction, and various high-speed movies of combustion data are available to validate the spray and combustion models [1-3,5-7,23-26].

Fuel Conditions	n-Heptane	n-Dodecane
Ambient temperature (K)	800–1300	900
Ambient density (kg/m^3)	14.8	22.8
Composition	Non-reacting: 0% O_2 Reacting: 10–21% O_2	Non-reacting: 0% O_2
Injection pressure (bar)	1500	1500
Fuel temperature (K)	373	363
Nozzle diameter (μm)	100	90
Duration of injection (ms)	6.8	1.5
Total mass injected (mg)	17.8	3.5
Fuel Density (kg/m^3)	700	750

Table 1: Range of conditions for the combusting spray experiments at Sandia National Laboratories [1-3,5-7,24-27,40] with n-heptane and n-dodecane.

Results and Discussion

Liquid penetration, vapor penetration, LOL, and ignition delay data will be used for validation of the turbulence models; hence, these parameters will be first defined, consistent with our previous investigations [4,29]. Liquid penetration is defined as the axial location encompassing 97% of the injected mass at that instant of time. Vapor penetration at any time is determined from the farthest downstream location of

0.05% fuel mass-fraction contour. Flame LOL is determined by the nearest upstream location of temperature ≥ 2200 K contour. Ignition delay is defined as the time from start of injection to the time when temperatures above 2000K are first observed in any computational cell.

Non-reacting Simulations

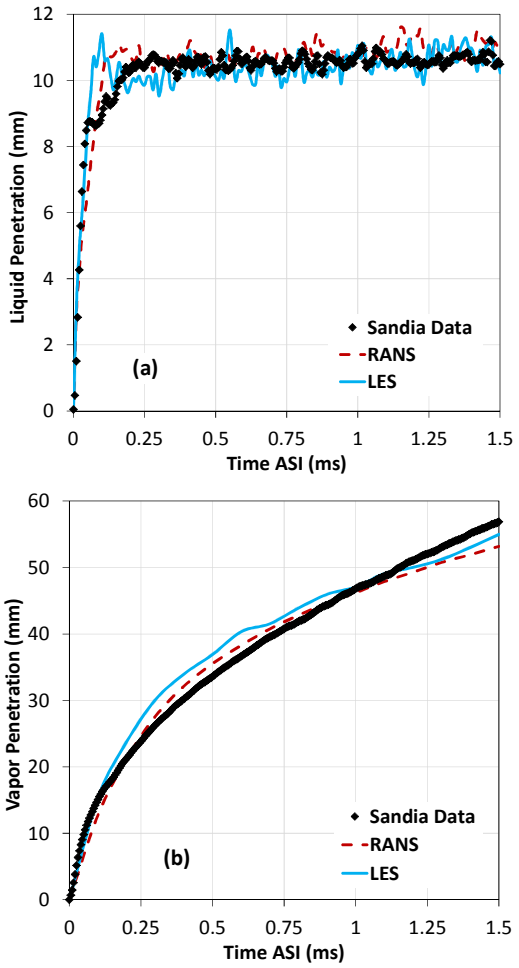

Figure 2: Measured [26,27] and predicted liquid penetration and vapor penetration vs. time for n-dodecane calculated by using RANS and LES turbulence models.

First, the non-reacting data-set is used for benchmarking the simulations to ensure that the fuel-air distribution is accurately predicted by the turbulence models. The reason for this is the fact that the fuel distribution (equivalence ratio) needs to be accurately predicted before combustion characteristics are validated. Figure 2 presents predicted and measured liquid spray and fuel vapor penetration at different times after start of injection (ASI) under non-reacting conditions for n-dodecane at an ambient temperature of 900K. The experimental conditions are listed in Table 1. The liquid and vapor penetration are better captured in the early stages (< 0.1 ms) by the LES model. However, the liquid length and vapor penetration is fairly well predicted by both the turbulence models. It should be noted that similar trends for liquid length and vapor penetration were also observed for n-heptane sprays, hence are not shown here. It can be concluded that global spray characteristics are well captured by both RANS and LES models.

The wall-clock time and maximum number of computational cells for RANS simulation are 2 hours and 150,000 cells respectively. The corresponding numbers for LES simulation are 20 hours and 2.1 million cells respectively. Both RANS and LES simulations were performed on 16 processors. Clearly, the increase in computational cost is significant for LES simulations. However, it should be noted that the main reason for this increase is the enhanced resolution of the flow field with 0.125 mm grid sizes using LES.

Further validation is performed against instantaneous contours of fuel distribution data for n-heptane fuel at an ambient temperature of 1000K [23,24]. The instantaneous experimental images obtained using Rayleigh scattering imaging are shown on the left along with the time ASI and the axial length scale (cf. Figs. 3 and 4). The field of view is 40 mm x 20 mm in the axial and transverse directions respectively. Note that the experimental contours pertain to a ratio between fuel-air number densities (N_f/N_a) and fuel-ambient air mixture temperature. Simulations plot the fuel mass-fractions and ambient gas temperatures respectively. Fuel vapor penetration and dispersion can be clearly seen from the experimental and simulation plots. Both RANS and LES simulations predict the vapor penetration fairly well. However, marked differences in the spray structure are clearly observed between RANS and LES cases. While RANS predicts smooth, averaged profiles, the LES simulation is able to capture the instantaneous structure well. However, the initiation of instabilities on the surface seems to be occurring further downstream in the case of LES compared to the experiments. Spray dispersion seems to be marginally underpredicted by the LES model. Early initiation of instabilities results in an early jet breakup which can enhance the spray and vapor dispersion as well. The vapor distribution also seems to be narrower for the LES model between the axial distances of 15 to 25 mm compared to the RANS model.

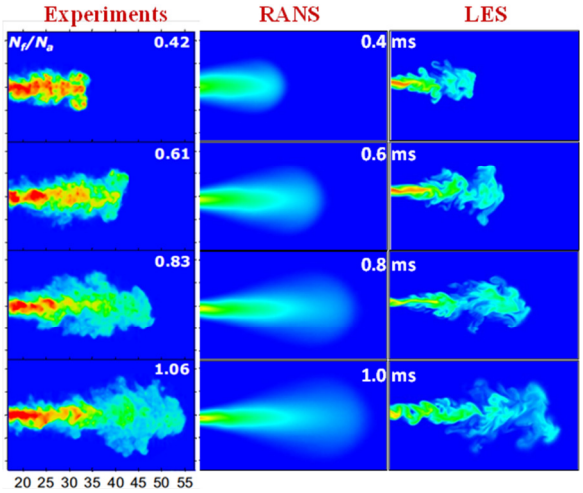

Figure 3: Images comparing the calculated equivalence ratio contours using RANS and LES models, against the experimental data from Sandia National Laboratory [24,25] under non-reacting conditions for NHPT fuel.

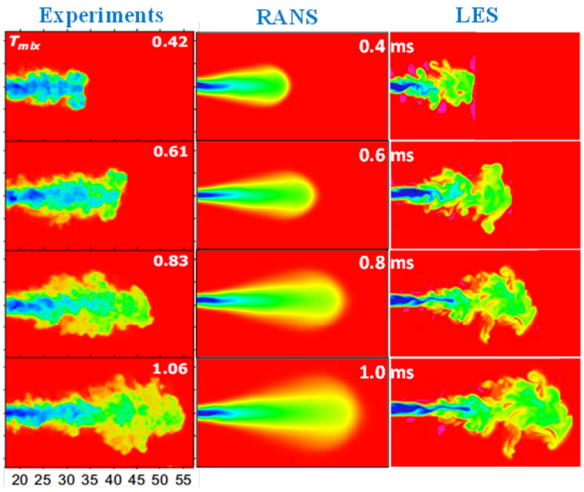

Figure 4: Images comparing the calculated temperature contours using RANS and LES models, against the experimental data from Sandia National Laboratory [24,25] under non-reacting conditions for NHPT fuel.

Figure 5 presents the mixture fraction distribution versus radial position for n-dodecane and n-heptane with RANS and LES turbulence models against data at different axial positions from the injector nozzle at 1.0 ms ASI. In experiments, the mixture fraction is calculated by using Rayleigh scattering. The fuel mass fraction was plotted for simulations because under non-reacting conditions, the mixture fraction is equivalent to the fuel mass fraction. At an axial location of 20 mm, both codes tend to under-predict the mixture fraction values, especially near the centerline. The fuel distribution is also narrower in the case of LES model which is consistent with observations in Fig. 3. At an axial location of 40 mm, the mixture fraction distribution is underpredicted by both the turbulence models. However, the LES model seems to perform better than the RANS model. It is well known that the Schmidt number value plays a significant role in vapor penetration and dispersion. Further studies need to be performed to quantify the influence of the turbulent Schmidt number on vapor penetration and dispersion results for both the turbulence models.

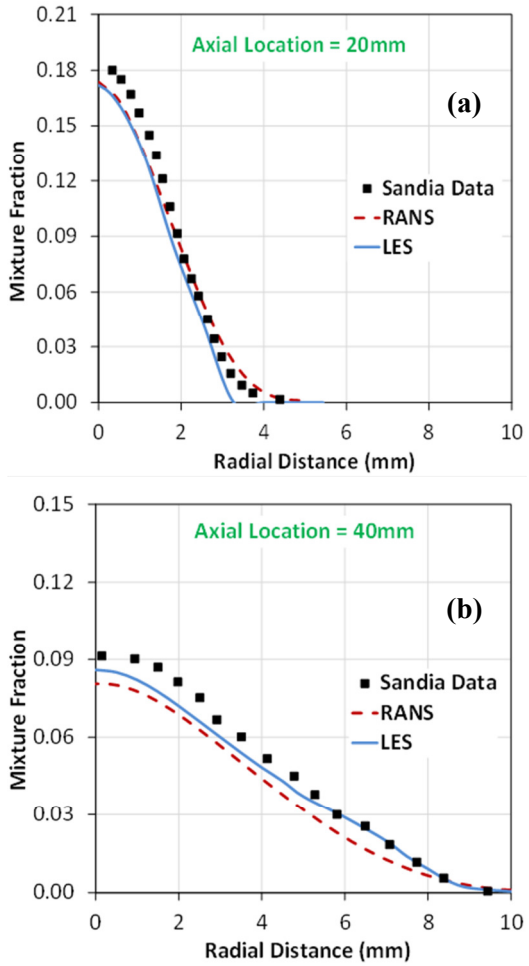

Figure 5: Measured [26,27] and predicted (using RANS and LES models) mixture fraction distribution versus radial distance for NHPT at different axial positions.

Figures 6 and 7 presents parametric studies on the influence of grid size and LES model constants on liquid penetration and vapor fraction contours. Figure 6 compares effect of grid size on liquid penetration length and vapor fraction contours using the LES model for cases corresponding to Fig. 2, de-

scribed in table 1. Three different grid sizes are tested i.e., 0.5 mm, 0.25 mm, and 0.125 mm. Figure 6a also plots the experimental data from Sandia [25,26]. The liquid penetration results improve qualitatively with grid refinement. The near nozzle spray penetration is also best captured by the 0.125 mm grid. The results for liquid penetration seem to be fairly grid independent beyond a minimum grid size of 0.25 mm.

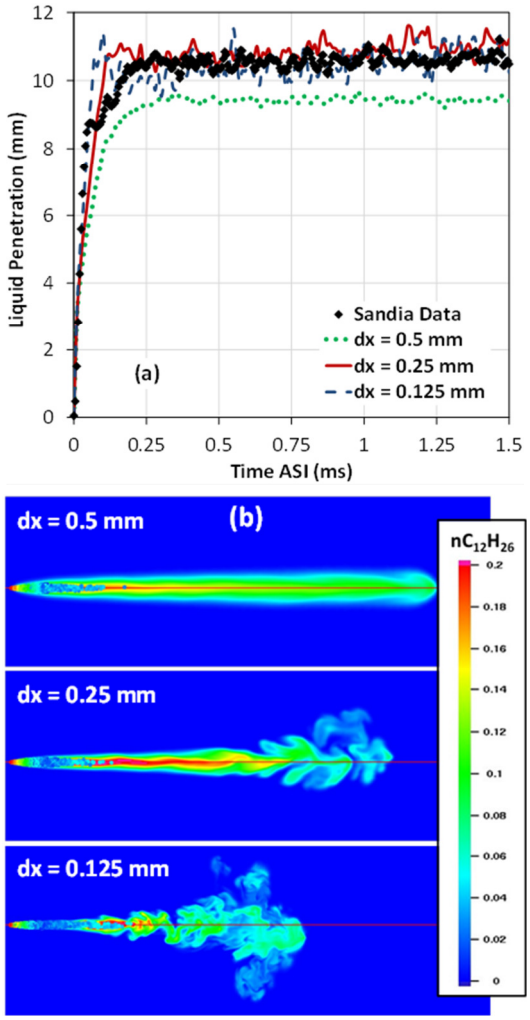

Figure 6: Effect of grid size on (a) liquid penetration vs. time, (b) vapor penetration contours at mid-plane at 1.0 ms ASI for LES using Smagorinsky model under non-reacting conditions with n-dodecane as fuel.

Figure 6b plots the vapor fraction contours at mid-plane at 1.0 ms ASI. The field of view is 75 mm x 25 mm in axial and radial directions, respectively. Although liquid penetration was observed to be fairly grid independent, vapor penetration contours are clearly grid dependent. Grid refinement results in more flow structures since the free shear instabilities which are Kelvin-Helmholtz based more towards the injector. The minimum grid size of 0.5 mm does not show any flow structures and behaves like a RANS simulation. It should be noted that Bharadwaj [37] observed flow structures with grid sizes of 0.5 mm and 0.67 mm. This is mainly due to the sub-grid scale model used. In our simulation, since Smagorinsky based LES model is implemented; it is not surprising that the large scale flow structures are not captured with a minimum grid size of 0.5 mm.

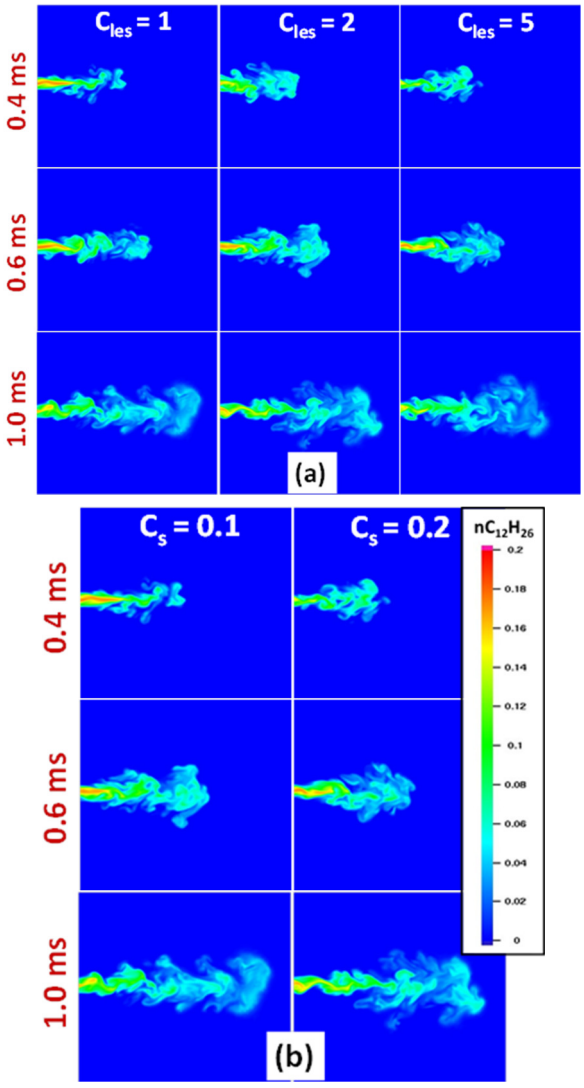

Figure 7: Effect of model constants on fuel vapor fraction contours at different times from ASI for LES with Smagorinsky model under non-reacting conditions with n-dodecane as fuel.

Figure 7 presents the influence of C_s and C_{les}, i.e., Smagorinsky based LES model constants on spray characteristics for cases discussed in the context of Figs. 2 and 6, with a minimum grid size of 0.125 mm. The vapor fraction contours are plotted at 0.4 ms, 0.6 ms, and 1 ms ASI. The field of view is 50 mm x 40 mm in axial and radial directions, respectively. Three different C_{les} values were tested, i.e., 1, 2, 5; and 2 different C_s values were evaluated i.e., 0.1, and 0.2. In general, for the range variation in C_s and C_{les}, liquid and vapor penetration lengths, liquid length results did not change appreciably (not plotted here). Vapor fraction contours also look quite similar as seen in Fig. 7.

Reacting Simulations

With the qualitative validation under non-reacting conditions, RANS and LES models are now compared under reacting conditions for NHPT. The test conditions simulated are shown in Table 1. Figure 8 presents the evolution of temperature contours with RANS and LES modeling approaches at an initial ambient temperature of 1000K. The white dashed line demarcates the predicted LOL at that time. The field of view is 100 mm x 60 mm in axial and radial directions, respectively. There are several interesting differences between the simulations:

(1) Ignition seems to occur earlier for the LES model with temperatures higher than 2000 K at 0.4ms. This is expected due to enhanced flow structure with the LES model.

(2) The temperature contours are smooth with the RANS model which is expected since it predicts a time-averaged mean value for the temporal variation. On the other hand, LES based on filtering rather than averaging can capture the temporal fluctuations of the same scale as the minimum grid size or higher.

(3) Volumetric auto-ignition is observed with the LES model, and the flame seems to be stabilized as a result of the spontaneous ignition phenomenon. However, with RANS the flame seems to be propagating upstream before being stabilized. This is also shown with the change in LOL at different times ASI. The RANS model shows that the LOL decreases with time; but the LES predicts only a minor change in LOL. Pickett et al. [38] have shown that flame stabilization seems to occur as a result of successive auto-ignition of the incoming fuel at the flame lift-off location rather than by flame propagation upstream. Hence, the results from the LES model clearly are more representative of the actual spray combustion process.

(4) Quasi-steady LOL values predicted by both models are very similar (not plotted here).

The wall-clock time and maximum number of computational cells for RANS simulation are 18 hours and 550,000 cells respectively. The corresponding numbers for LES simulation are 150 hours and 3.5 million cells respectively, at 2 ms ASI. Both RANS and LES simulations were performed on 24 processors. Clearly, the increase in computational cost is significant for performing LES simulations. However, it should be noted that the main reason for this increase is the enhanced resolution of the flow field with 0.125 mm grid sizes using LES.

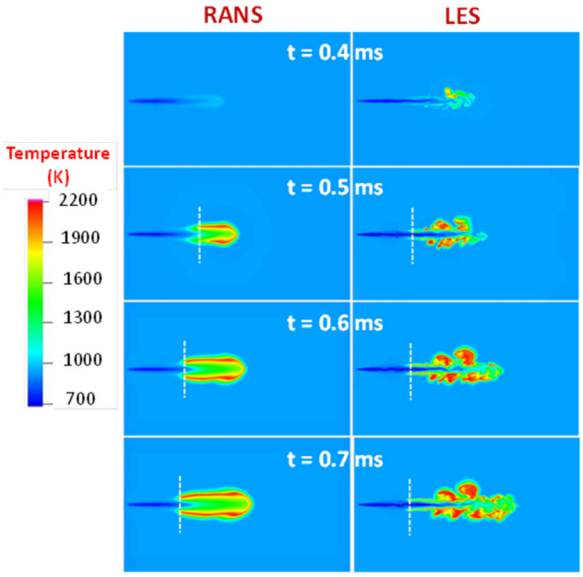

Figure 8: Comparison of predicted temperature contours calculated using RANS and LES turbulence models, respectively, at different times ASI using n-heptane as fuel.

In Fig. 9, quantitative comparisons of predicted ignition delays at different ambient temperatures and oxygen concentrations by RANS and LES turbulence models are presented. The data for NHPT were obtained at Sandia [26]. It is clear that the LES model predicts lower ignition delay values which is perhaps because of the enhanced flow structures. Also, under the conditions investigated it seems that the LES model performs marginally better than the RANS model in predicting ignition delays at different ambient temperatures. Flame LOL validation is not presented since the quasi-steady LOL value predicted by the RANS and LES models were close and both agree very well with the experimental data.

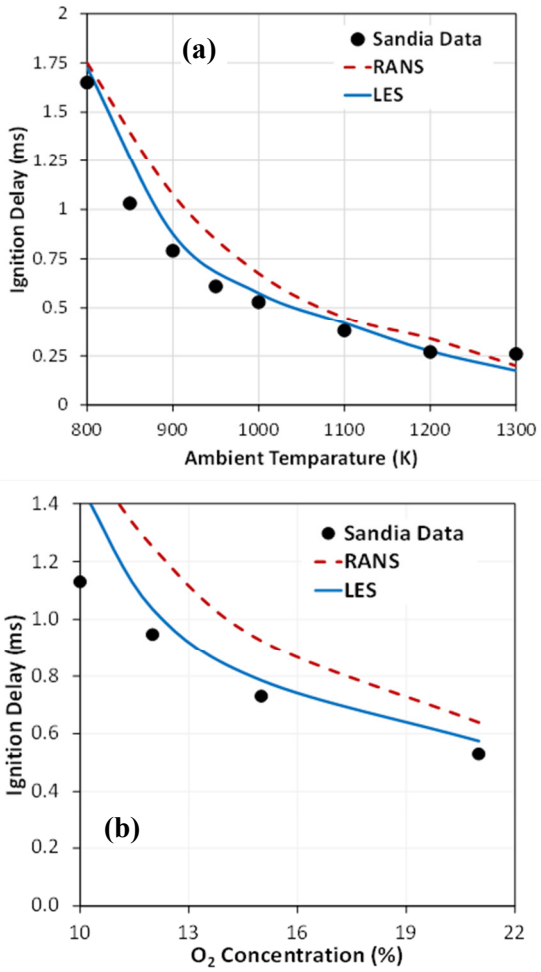

Figure 9: Measured [3,5,27] and predicted ignition delay vs. (a) ambient temperature, (b) oxygen concentration, for NHPT calculated by using RANS and LES turbulence models.

Planar laser-induced incandescence (PLII) images of soot [6,7] along a thin plane of the fuel jet were compared with model predictions by RANS and LES in Fig. 10. Time ASI for each image is shown on the left thus the temporal evolution of a typical combustion event is seen. Distance from the injector is shown at the bottom while the dashed and solid vertical lines represent LOL (19mm) and an axial position of 50mm respectively. The soot mass production within a computation cell is determined from a single-step competition between formation and oxidation rates of C_2H_2 species, based on the Hiroyasu model [39]. The soot formation rate depends on the formation C_2H_2 species which is a precursor for soot production. Soot oxidation is modeled using Nagle and Strickland-Constable correlations assuming the soot particles to be spherical and uniform in size. Further details about the soot model can be found in the references [29,39]. This soot model has been extensively used in the literature. It can be seen that the predicted soot distributions agree well with the experimental results. The experimentally observed trend that soot generation occurs beyond the LOL is also well captured by both RANS and LES models. The instantaneous structure of soot though is better captured by the LES model. The RANS model on the other hand provides an averaged soot distribution contour. These results are consistent with findings in Figs. 3 and 4 that the instantaneous flow structures are better predicted by the LES model.

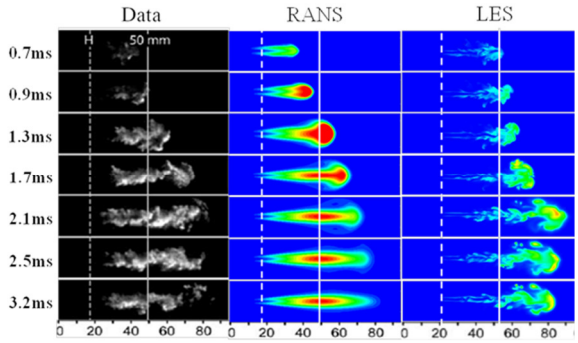

Figure 10: Time sequence of PLII images and predicted soot mass fraction contours [6,7,40] by using RANS and LES turbulence models.

Conclusions

This study focused on evaluating the use of a Smagorinsky-based LES turbulence model. The constant volume combustion data from Sandia National Laboratory was extensively used for validation purposes. The high resolution LES model was compared against a standard RANS model which is currently used by the industry. The main objectives of the study being to identify the potential benefits of using a LES model and the associated increase in computational cost. The following conclusions can be drawn:

1) Global spray and combustion characteristics such as liquid and vapor penetration, mixture fraction, liquid length, and flame LOL are well captured by both RANS and LES models.
2) Instantaneous equivalence ratio, temperature and soot contours are better captured by the LES model. This is mainly due to the fact that the LES model is able to capture the large scale flow structures.
3) Predicted ignition delay is lower with the LES model which is expected. This results in improved

agreement with experimental data from Sandia National Laboratory for NHPT fuel.

4) Under certain conditions investigated the LES model provides improved qualitative and quantitative predictions. However these are associated with a significant increase in computational cost. This increase is mainly attributed to the need for higher resolution with a Smagorinsky based LES model.
5) The grid size has a significant influence on vapor fraction contours; however, liquid penetration seems to be fairly grid independent. Other LES model constants do not influence the spray characteristics appreciably.
6) The LES model also predicts volumetric auto-ignition and a fairly stabilized LOL, which is more realistic under the conditions investigated. In contrast, the RANS model predicts ignition kernels moving upstream, which is inconsistent with the experimental results from Sandia.

ACKNOWLEDGMENTS

The submitted manuscript has been created by UChicago Argonne, LLC, operator of Argonne National Laboratory (Argonne). Argonne, a U.S. Department of Energy Office of Science laboratory, is operated under Contract No. DE-AC02-06CH11357. The U.S. Government retains for itself, and others acting on its behalf, a paid-up, nonexclusive, irrevocable worldwide license in said article to reproduce, prepare derivative works, distribute copies to the public, and perform publicly and display publicly, by or on behalf of the Government.

NOMENCLATURE

C_s	Smagorinsky model constant (= 0.1-0.2)
C_{les}	LES Model constant (= 1-5)
F_i	Source term due to drag on droplets [Pa]
P	Pressure of gas mixture [Pa]
S_{ij}	Symmetric stress tensor [m^2/s^2]
T_{ij}	LES sub-grid scale tensor [m^2/s^2]
V_{cell}	Cell volume [m^3]
u	Gas velocity [m/s]
Δ	Filter size [m]
δ	Kronecker delta
k	Sub-grid turbulent kinetic energy [m^2/s^2]
μ	Dynamic Viscosity [Pa.s]
ρ	Density of the gas mixture [kg/m^3]

ABBREVIATION

ASI	After start of injection
LES	Large eddy simulation
LOL	Lift-off length
PLII	Planar laser-induced incandescence
RANS	Reynolds-averaged Navier-Stokes

REFERENCE

1. Naber, J.D., Siebers, D.L., 1996, "Effects of gas density and vaporization on penetration and dispersion of diesel sprays", SAE Paper No. 960034.
2. Higgins, B.S., Siebers, D.E., 2001, "Measurement of the Flame Lift-off Location on DI Diesel Sprays Using OH Chemiluminescence", SAE Paper No. 2001-01-0918.
3. Siebers, D.L., Higgins, B.S., "Flame Lift-off on Direct-Injection Diesel Sprays under Quiescent Conditions", SAE Paper No. 2001-01-0530.
4. Som, S., Aggarwal, S.K., 2010, "Effects of primary breakup modeling on spray and combustion characteristics of compression ignition engines", Combustion and Flame, Vol. 157, pp.1179-1193.
5. Siebers, D.L., 1998, "Liquid-phase fuel penetration in diesel sprays", SAE Paper No. 980809.
6. Pickett, L.M., Siebers, D.L., 2004, "Soot in diesel fuel jets: effects of ambient temperature, ambient density, and injection pressure", Combustion and Flame, Vol. 138, pp. 114-135.
7. Pickett, L.M., Siebers, D.L., 2002, "An investigation of diesel soot formation processes using micro-orifices", Proceedings of the Combustion Institute, Vol. 29, pp. 655-662.
8. Faeth, G.M., 1987, "Mixing, transport and combustion in sprays", Progress in Energy and Combustion Science, Vol. 13 (4), pp. 293-345.
9. Sirignano, W.A., 2005, "Volume averaging for the analysis of turbulent spray flows", International Journal of Multiphase flow, Vol. 31 (6), 675-705.
10. Pope, S.B., 2000, "Turbulent Flows", Cambridge University Press.
11. Senecal, P.K., Pomraning, E., Richards, K.J., 2003, "Multi-Dimensional Modeling of Direct-Injection Diesel Spray Liquid Length and Flame Lift-off Length using CFD and Parallel Detailed Chemistry", SAE Paper No. 2003-01-1043.
12. Kong, S.C., Sun, Y., Reitz, R.D., 2007, "Modeling Diesel Spray Flame Lift-off, Sooting Tendency, and NOx Emissions Using Detailed Chemistry with Phenomenological Soot Model", Journal of Gas Turbine and Power, Vol. 129, pp. 245-251.

13. Som, S., Ramirez, A.I., Aggarwal, S.K., Kastengren, A.L., El-Hannouny, E.M., Longman, D.E., Powell, C.F., Senecal, P.K., 2009, “Development and Validation of a Primary Breakup Model for Diesel Engine Applications”, SAE Paper No. 2009-01-0838.
14. Lucchini, T., D’Errico, G.D., Ettore, D., Ferrari, G., 2009, “Numerical investigation of non-reacting and reacting diesel sprays in constant-volume vessels”, SAE Paper No. 2009-01-1971.
15. Azimov, U., Kawahara, N., Tomita, E., Tsuiboi, K., 2010, “Evaluation of the flame lift-off length in diesel spray combustion based on flame extinction”, Journal of Thermal Science and Technology, Vol. 5 (2), pp. 238-251.
16. Venugopal, R., Abraham, J., 2007, “A numerical investigation of flame lift-off in diesel jets”, Combustion science and technology, Vol. 179, pp. 2599-2618.
17. Karrholm, F.P., Tao, F., Nordin, N., 2008, “Three-Dimensional Simulation of Diesel Spray Ignition and Flame Lift-off Using OpenFOAM and KIVA-3V CFD Codes”, SAE Paper No. 2008-01-0961.
18. Rutland, C.J., 2011, “Large-eddy simulations for internal combustion engines – a review”, International Journal of Engine Research, Vol. 12 (5), pp. 421-451.
19. Pomraning, E., 2000, “Development of large eddy simulation turbulence models”, Ph.D. thesis, University of Wisconsin - Madison.
20. Pomraning, E., Rutland, C.J., 2002, “Dynamic one-equation non viscosity large-eddy simulation model”, AIAA Journal, 40(4), pp. 689-701.
21. Banerjee, S., Liang, T., Rutland, C., Hu, B., 2010, “Validation of an LES multi model combustion model for diesel combustion”, SAE Paper No. 2010-01-0361.
22. Smagorinsky, J., 1963, “General circulation experiments with the primitive equations”, Monthly Weather Review.
23. Idicheria, C.A., Pickett, L.M., 2007, “Effect of EGR on diesel premixed-burn equivalence ratio”, Proceedings of the Combustion Institute, Vol. 31, pp. 2931-2938.
24. Idicheria, C.A., Pickett, L.M., 2007, “Quantitative mixing measurements in a vaporizing diesel spray by Rayleigh imaging”, SAE Paper No. 2007-01-0647.
25. Pickett, L.M., Manin, J., Genzale, C.L., Siebers, D.L., Musculus, M.P.B., Idicheria, C.A., 2011, “Relationship between diesel fuel spray vapor penetration/dispersion and local fuel mixture fraction”, SAE Paper No. 2011-01-0686.
26. http://www.sandia.gov/ecn/
27. Senecal, P.K., Richards, K.J., Pomraning, E., Yang, T., Dai, M.Z., McDavid, R.M., Patterson, M.A., Hou, S., Sethaji, T., 2007, “A new parallel cut-cell Cartesian CFD code for rapid grid generation applied to in-cylinder diesel engine simulations”, SAE Paper No. 2007-01-0159.
28. Richards, K.J., Senecal, P.K., Pomraning, E., 2008, CONVERGE™ (Version 1.2) Manual, Convergent Science, Inc., Middleton, WI.
29. Som, S., 2009, “Development and Validation of Spray Models for Investigating Diesel Engine Combustion and Emissions;” PhD thesis, University of Illinois at Chicago.
30. Reitz, R.D., 1987, “Modeling Atomization Processes in High Pressure Vaporizing Sprays”, Atomization and Spray Technology, Vol. 3, pp. 309-337.
31. Patterson, M.A., Reitz, R.D., 1998, “Modeling the Effects of Fuel Spray Characteristics on Diesel Engine Combustion and Emissions”, SAE Paper No. 980131.
32. Schmidt, D.P., Rutland, C.J., 2000, “A New Droplet Collision Algorithm”, Journal of Computational Physics, Vol. 164, pp. 62-80.
33. Post, S.L., Abraham, J., 2002, “Modeling the outcome of drop-drop collisions in diesel sprays”, International Journal of Multiphase Flow, Vol. 28, pp. 997-1019.
34. Lu, T. F., Law, C.K., Yoo, C.S., Chen J.H., 2009, "Dynamic Stiffness Removal for Direct Numerical Simulations", Combustion and Flame, Vol. 156 (8), pp.1542-1551.
35. Haworth, D.C., 2010, “Progress in probability density function methods for turbulent reacting flows”, Progress in Energy and Combustion Science, Vol. 36, pp. 168-259.
36. S. Bhattacharjee, J. Jaishree, V. Raj Mohan, H. Zhang, Haworth, D.C., 2011, “PDF-based simulations of turbulent spray combustion in a constant-volume chamber”, Eastern States Section of the Combustion Institute, University of Connecticutm Storrs, October 2011.
37. Bharadwaj, N., 2010, “Large eddy simulation turbulence modeling of spray flows”. Ph.D. thesis, University of Wisconsin-Madison.
38. Pickett, L.M., Kook, S., Persson, H., Andersson, O., 2009, “Diesel fuel jet lift-off stabilization in the presence of laser-induced plasma ignition”, Proceedings of the Combustion Institute, Vol. 32, pp. 2793-2800.
39. Heywood, J.B., 1998, “Internal Combustion Engine Fundamentals”. McGraw-Hill, Inc.